Strain-Induced Insulator State and Giant Gauge Factor of $La_{0.7}Sr_{0.3}CoO_3$ Films

A. D. Rata,[1] A. Herklotz,[1] K. Nenkov,[1,2] L. Schultz,[1] and K. Dörr[1]

[1]*IFW Dresden, Institute for Metallic Materials, Helmholtzstraße 20, 01069 Dresden, Germany*

[2]*International Laboratory of High Magnetic Fields and Low Temperatures, PL-53421 Wroclaw, Poland*

(Received 13 November 2007; published 20 February 2008)

A strain-induced change of the electrical conductivity by several orders of magnitude has been observed for ferromagnetic $La_{0.7}Sr_{0.3}CoO_3$ films. Tensile strain is found to drive the narrow-band metal highly insulating. Reversible strain applied using a piezoelectric substrate reveals huge resistance modulations including a giant piezoresistive gauge factor of 7000 at 300 K. Magnetization data recorded for statically and reversibly strained films show moderate changes. This indicates a rather weak strain response of the low-temperature Co spin state. We suggest that a strain-induced static Jahn-Teller–type deformation of the CoO_6 units may provide a localization mechanism that also has impact on electronic transport in the paramagnetic regime.

DOI: 10.1103/PhysRevLett.100.076401 PACS numbers: 75.80.+q, 71.27.+a, 71.30.+h, 85.80.Jm

The electronic properties of a number of 3*d* transition metal (TM) oxides are unusually sensitive to external parameters like electromagnetic fields or mechanical strain. This gives access towards controlling their electrical conductivity, offering substantial potential for future oxide electronics. General reasons for this sensitivity are the presence of both strong electron correlation and electron-phonon interaction. The effective width of the TM 3*d* bands is typically low in these materials and, thus, electron transport is particularly susceptible to localization phenomena.

The most prominent example concerns doped lanthanum manganites showing the colossal magnetoresistance (CMR) in large magnetic fields [1–4]. While manganites are also sensitive to mechanical strain (pressure, epitaxial strain in films) [5–8], an even larger strain response of electrical transport is described here for a compound from the related family of $La_{1-x}Sr_xCoO_3$. Recently, the electrical conductivity of metallic $La_{0.82}Sr_{0.18}CoO_3$ single crystals was found to drop under hydrostatic pressure, leading to an insulator state [9]. This effect is related to an additional degree of freedom: the Co^{3+} d^6 and Co^{4+} d^5 ions may display various (low, intermediate, and high) spin states due to a delicate balance between the crystal-field splitting Δ_{CF} and the intra-atomic Hund exchange [10]. Since Δ_{CF} is very sensitive to the variation of the Co-O bond length [11,12], structural changes can modify the Co spin state.

In the ground state, the parent compound $LaCoO_3$ is a nonmagnetic insulator with a low-spin (LS, $S = 0$) configuration. It is thermally excited to either an intermediate-spin (IS, $S = 1$) or a high-spin (HS, $S = 2$) state above $T \approx 100$ K and becomes a metal above 400 K [10,12]. Doping $LaCoO_3$ with a divalent metal creates Co^{4+} ions, triggering itinerant ferromagnetic double exchange (DE) interactions with the adjacent IS Co^{3+} ions [13,14]. Doped with Sr^{2+}, the material is a ferromagnetic cluster glass for $x > 0.18$ [13,15]. At about the same doping level, the system gets metallic. At lower doping, conducting hole-rich clusters coexist with an insulating Co^{3+} rich matrix [13,16–18]. We note that only the IS state of Co^{3+} is Jahn-Teller active and doped cobaltites show a mixture of spin states at temperatures below 300 K [14,19]. $La_{0.7}Sr_{0.3}CoO_3$ films have been employed as electrodes for ferroelectric capacitors and in high-temperature applications as catalysts and ionic conductors. The magnetic properties of low-strain $La_{0.7}Sr_{0.3}CoO_3$ films have been studied by Fuchs *et al.* [20]. However, to our knowledge, systematic studies of strain-dependent properties in films are lacking.

We investigate the influence of biaxial epitaxial strain on the electrical resistance (R) and the magnetization (M) of $La_{0.7}Sr_{0.3}CoO_3$ films. Films that are 60 nm thick are found to grow coherently under compressive (tensile) strain on $LaAlO_3$ ($SrTiO_3$) substrates. The direct strain effect on R and M is recorded using films grown epitaxially on a pseudocubic piezoelectric substrate. The conductivity of differently strained films is found to differ by more than 5 orders of magnitude at 300 K and the films under tensile strain are highly insulating. Measurements under reversible strain confirm the extreme strain sensitivity of the electrical conductivity. In contrast, M data show a moderate strain response. We suggest that biaxial strain may induce a static Jahn-Teller–type lattice distortion, which may be efficient as a localization mechanism.

$La_{0.7}Sr_{0.3}CoO_3$ (LSCO) films were grown on single-crystalline substrates of $SrTiO_3(001)$ (STO), $LaAlO_3(001)$ (LAO), and $Pb(Mg_{1/3}Nb_{2/3})_{0.72}Ti_{0.28}O_3(001)$ (PMN-PT) by pulsed laser deposition (KrF 248 nm) from a stoichiometric target. The deposition temperature and the oxygen background pressure were 650 °C and 3.5×10^{-1} mbar, respectively. The films were cooled down in 600 mbar of oxygen. Structural characterization has been carried out using a Philips X'Pert MRD diffractometer with Cu $K\alpha$ radiation. The magnetization was measured in a SQUID magnetometer. Electrical transport measurements were performed using a standard four-terminal technique. In

recent work [7,21] we demonstrated the reversible control of biaxial in-plane strain in films grown epitaxially on piezoelectric PMN-PT(001). The substrate strain is controlled by an electrical voltage applied between the conducting film and a bottom electrode on the opposite face of the substrate [Fig. 3(a), inset]. If the LSCO films had too high resistance for the proper function as an electrode, large area Pt electrodes were deposited on top. The employed PMN-PT has a rhombohedral lattice structure similar to that of LAO, apart from the larger lattice parameter of 4.02 Å, and provides a rather uniform in-plane strain.

LSCO films have been epitaxially grown in three distinct strain states on STO, LAO, and PMN-PT substrates. In Fig. 1(a) we show the wide angle $\Theta - 2\Theta$ x-ray diffractograms (XRD) of 60 nm thick films grown on LAO (top) and STO (bottom). The films display clear (00l) reflections of the pseudocubic structure with no indications of impurities or misorientation. The film grown on LAO (STO) is under in-plane compressive (tensile) strain. In Fig. 1(b) we compare the XRD reciprocal space maps around the nonspecular (013) reflection of these films. In either case, the same Q_x value is found for both film and substrate, proving the coherently strained growth of LSCO (60 nm) on LAO and STO. The pseudocubic in-plane lattice parameter is $a = 3.78$ Å (3.90 Å) for the film on the LAO (STO) substrate, compared to 3.82 Å [16] for bulk LSCO. In Table I, lattice parameters of three different films (including one on PMN-PT) and their tetragonal distortion estimated as $t = 2(a - c)/(a + c)$ are listed. The tetragonal distortion of the films spans a wide range from -2.3% (LAO) to 1.8% (PMN-PT) and 3.1% (STO). LSCO/PMN-PT films are epitaxially but not coherently grown.

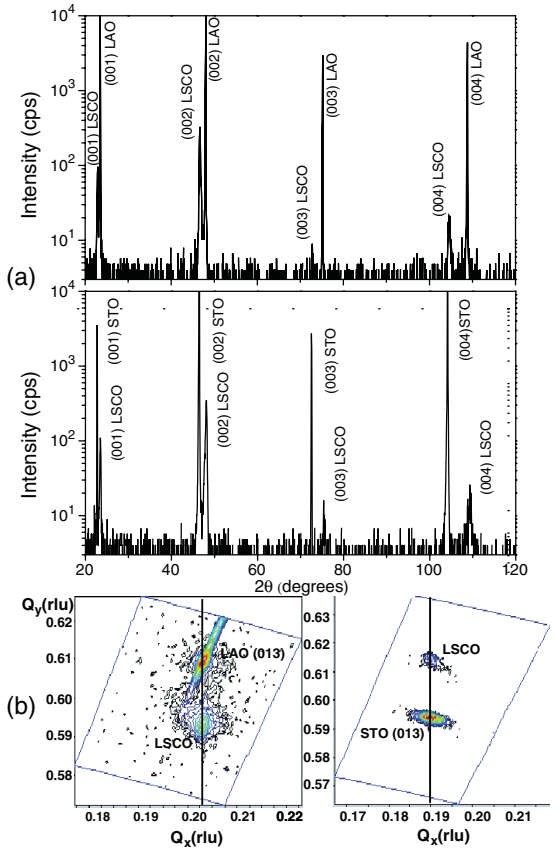

FIG. 1 (color online). (a) $\Theta - 2\Theta$ X-ray diffractograms of 60 nm thick LSCO films on LAO (top) and STO (bottom) substrates. (b) XRD reciprocal space map around the (013) reflection for the same LSCO films on LAO (left) and STO (right).

A drastic effect of the varied strain is observed in the electrical transport of the LSCO films. In Fig. 2, we present the temperature dependence of the resistivity (ρ) under in-plane compression or expansion. The LSCO/LAO film displays metallic conductivity at all temperatures, which is similar to the bulk behavior, e.g., $\rho(5\ \mathrm{K}) \simeq 1.2 \times 10^{-4}\ \Omega\,\mathrm{cm}$ [13,22]. In contrast, the LSCO/PMN-PT film with medium tensile strain displays an insulating behavior with $\rho(300\ \mathrm{K}) \simeq 40\ \Omega\,\mathrm{cm}$. The LSCO/STO film with larger tensile strain had a gigaohm resistance at 300 K (not shown). This result of extremely enhanced resistance has been reproduced for a number of films. We argue that this strikingly large conductivity variation among the films is essentially caused by strain. Images taken by atomic force microscopy show reasonably smooth films with a roughness (rms) of about 1 nm. Insulating behavior caused by microcracks is ruled out based on (i) a decrease of ρ observed for increasing film thickness, (ii) negligible strain relaxation (film on STO), and (iii) the linear current-voltage characteristics of the films.

Transport data measured as a function of reversible substrate strain give direct evidence for an extreme strain sensitivity of the LSCO films. In Fig. 3(a), R vs the electric field (E) applied to the piezoelectric substrate is plotted for 300 K. The substrate produces a compression of about 0.15% for $E = 15\ \mathrm{kV/cm}$. R reveals a reversible, giant modulation by a factor close to 10. The maxima are located at the ferroelectric coercive fields of the substrate. The large hysteresis originates from the film, since the substrate strain is weakly hysteretic [7]. Similar data recorded near T_C show a R modulation by a factor of $\simeq 3$. In order to exclude charging effects, the measurements were performed at various speeds. A giant gauge factor (denoting the ratio of percental changes of R and the strain) of 7000 is derived from the 300 K data. Since this huge strain effect is observed far above T_C, it implies promising opportunities for applications. We further note that, apart from the much

TABLE I. In-plane (a) and out-of-plane (c) lattice parameters of LSCO films, the tetragonal distortion t defined as $2(a - c)/(a + c)$, and the Curie temperature T_C. a_{sub} denotes the pseudocubic substrate lattice parameter.

LSCO films (60 nm)	a_{sub} (Å)	c (Å)	a (Å)	t	T_C (K)
LSCO/LAO	3.78	3.87	3.78	−2.3%	194
LSCO/STO	3.905	3.78	3.90	+3.1%	195
LSCO/PMN-PT	4.02	3.79	3.86	+1.8%	200

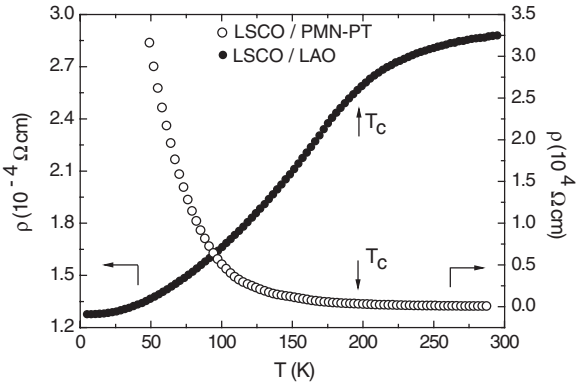

FIG. 2. Temperature dependence of the resistivity of LSCO/LAO (left scale) and LSCO/PMN-PT (right scale) films of 60 nm thickness.

larger magnitude of the present effect, the decrease of R with reduced tensile strain agrees with the observations for $La_{0.7}Sr_{0.3}MnO_3$ films [7].

Here, it is necessary to consider the influence of compositional differences among the films, since tensile strain could cause oxygen deficiency or Sr enrichment. Higher Sr doping drives the films more conducting, opposite to the observations. Since bulk $La_{1-x}Sr_xCoO_3$ shows oxygen deficiency for $x > 0.5$, underoxygenation as a consequence of tensile strain cannot be ruled out. However, a careful check of the literature on bulk cobaltites reveals that a similarly large ρ as for our films is never detected. For bulk $La_{0.7}Sr_{0.3}CoO_{2.85}$, $\rho(300\ \mathrm{K}) \simeq 6 \times 10^{-4}\ \Omega\,\mathrm{cm}$ and metallic conduction is reported [23]. Even an undoped crystal of $LaCoO_3$ with $\rho(300\ \mathrm{K}) \simeq 10\ \Omega\,\mathrm{cm}$ would correspond to a film of 400 kΩ in our measuring geometry, and slight doping by 0.2% of Sr reduces ρ by a factor of 10 [24]. Combined with the recorded huge gauge factor, these facts clearly indicate a mechanism different from oxygen deficiency for the conductivity variation.

Unlike the electrical transport, the magnetization of the LSCO films is moderately influenced by the strain. The temperature-dependent M of the LSCO/LAO and LSCO/STO films from Table I is plotted in Fig. 4. Data were recorded during warming in a magnetic field of 100 mT after field cooling (FC) or zero-field cooling (ZFC). The T_C values estimated by extrapolating M^2 for $T < T_C$ to $M = 0$ are given in Table I. They are somewhat lower than the bulk value of 225 K [17,22], but our M data agree with those reported by Fuchs *et al.* [20] for low-strain films, indicating a finite size effect on T_C. The pronounced branching between the ZFC and FC curves in Fig. 4 is known from the bulk phase and has been attributed to a magnetic cluster-glass state [13,15]. There is no significant difference in the FC curves of the two films, but a higher ZFC magnetization is observed for the LSCO/LAO film. M loops recorded at 10 K exhibit strongly enhanced coercive fields H_C as compared to bulk LSCO, of 880 mT (440 mT) for the film on STO (LAO) (Fig. 4, inset). Metallic conduction leads to a ferromagnetic coupling contribution in the framework of DE for the film on LAO, possibly underlying its higher M_{ZFC} and lower H_C, but the origin of the large H_C in the films needs further investigation. The calculated magnetic moments per Co at 10 K of the two films differ by less than 10%. Although this estimation is subject to errors from film thickness and microstructure, it indicates a minor spin state variation of Co ions among the films. We also recorded the direct strain response of M of a 30 nm thick LSCO/PMN-PT film. A continuous increase of M is observed with the piezoelectric compression in the film plane [Fig. 3(b), inset], i.e., with reduced tetragonality in the film. Interestingly, this is analogous to the strain effect on M in $La_{0.7}Sr_{0.3}MnO_3$ [7]. The temperature dependence of the relative change of M obtained by applying 14 kV/cm to the substrate is shown in Fig. 3(b). The strain

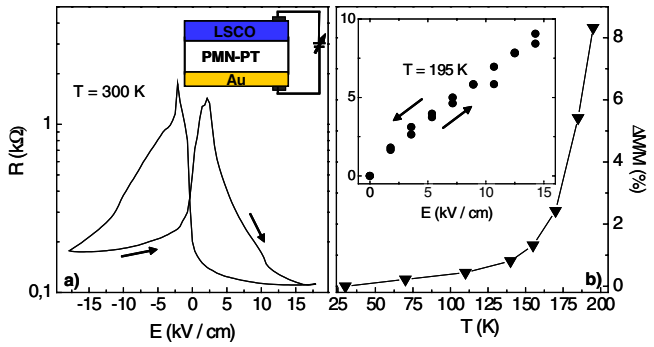

FIG. 3 (color online). (a) Resistance vs the electric field (E) applied to the piezoelectric substrate for a 60 nm LSCO/PMN-PT(001) film ($E \parallel [001]$). Inset: device scheme for reversible strain application. The piezoelectric in-plane compression grows roughly linearly with E. (b) Temperature dependence of the strain-induced magnetization (M) change calculated as $[M(E) - M(0)]/M(0)$ at $E = 14$ kV/cm for a 30 nm thick film. Inset: $[M(E) - M(0)]/M(0)$ vs E at 195 K. M is recorded in FC mode in $\mu_0 H = 100$ mT along [100].

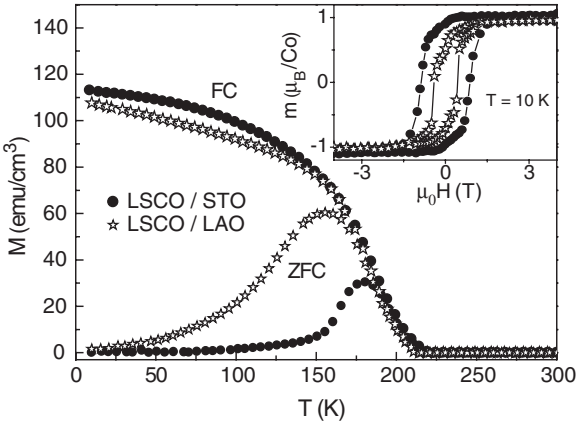

FIG. 4. Temperature-dependent in-plane magnetization of strained LSCO films measured in both FC and ZFC modes in a field of 100 mT along the [100] substrate direction. Inset: magnetic hysteresis loops at 10 K.

response peaks near T_C and vanishes for $T \ll T_C$. (The piezoelectric strain of the substrate decreases by a factor of about 2 between 300 K and 90 K.)

In the following, the origin of the strain-induced insulator state is considered. The pressure-induced insulator state in $La_{0.82}Sr_{0.18}CoO_3$ is due to an enhancement of the crystal-field splitting, driving Co^{3+} ions into the LS state and depleting the e_g conduction band [9]. This mechanism is unlikely for the present experiment. The enlarged in-plane lattice parameter of films under tensile strain is rather expected to reduce Δ_{CF}. Additionally, the tetragonal distortion could result in further reduction of the separation between the upper t_{2g} and lower e_g levels. Thus, tensile strain may increase the number of IS or HS Co ions in a cobaltite film, opposite to hydrostatic pressure. Still, for the investigated doping level, $x = 0.3$, the spin state of the Co ions seems to be less sensitive to strain at temperatures below T_C, since little strain-dependent variations of M are found. Further, M increases in the direct strain experiment when reducing the tensile strain [Fig. 3(b)], contrary to the expectation for a strain-induced increase in the number of IS or HS Co ions.

A microscopic mechanism that may be responsible for electron localization under tensile film strain is a strain-induced cooperative Jahn-Teller–type (JT) distortion. The tetragonal distortion of close-to-cubic unit cells caused by the strain is likely to have two effects: (i) suppression of the itinerant DE [5], and (ii) a cooperative JT-type distortion of the CoO_6 octahedra associated with favored in-plane e_g $d_{x^2-y^2}$ orbital occupation [5,6,8,14,25]. Both, in particular, the cooperative JT distortion, are efficient localization mechanisms for e_g electrons in ferromagnetic manganites [1–3,6,8]. Cobaltites show an additional spin state and electronic transition above 400 K [12,13,24] that may well be influenced by a JT-type distortion. Hence, this instability may be related to the observed high-temperature strain sensitivity in cobaltites. The importance of the same effects (i) and (ii) as in ferromagnetic manganites is supported by the fact that the same signs of dM/dt and dR/dt with respect to a tetragonal distortion t of the unit cells are recorded for $La_{0.7}Sr_{0.3}MO_3$ (M = Mn or Co) [7]. However, magnitudes are strikingly different, revealing a much stronger (weaker) reaction of R (M) towards the strain in the cobaltite.

There is strong evidence for a coexistence of hole-rich metallic (ferromagnetic, for $T < T_C$) and hole-poor insulating (magnetically less-ordered) clusters in $La_{0.7}Sr_{0.3}CoO_3$ [14,16,18,19,26]. An externally controlled cluster percolation is known to trigger extreme changes of the electrical conductivity in the framework of CMR [1,2]. Hence, a percolation scenario may underlie the huge variation in conductivity for our differently strained films, which is, on the other hand, accompanied by moderate variation of magnetization. At this point we note the rather weak doping dependence of T_C in bulk $La_{1-x}Sr_xCoO_3$, i.e., 220 K $< T_C <$ 270 K for $0.2 < x < 0.9$ [13,27]. An inhomogeneous cluster state with an intracluster-dominated T_C could be at the origin of both, the moderate strain and doping dependences of T_C.

To conclude, the electrical conductivity and magnetization of $La_{0.7}Sr_{0.3}CoO_3$ films have been investigated in various static and in reversible strain states. An extremely enhanced resistivity is observed under tensile biaxial strain. Strain-dependent data obtained using a piezoelectric substrate reveal piezoresistive gauge factors up to 7000, which exceed those detected for semiconducting carbon nanotubes [28]. Since this giant elastoresistance is also observed in the paramagnetic state of a lanthanum cobaltite, this compound family may allow one to overcome some of the restrictions for application that result from a low T_C. At present, reliable *ab initio* calculations and spectroscopic experiments are highly desirable to clarify the influence of the lattice parameters on the electronic structure and the spin state.

We thank D. Khomskii, M. Richter, L. Hozoi, V. Kataev, K. H. Müller, H. Tjeng, M. Fiebig, H. M. Christen, and L. Eng for fruitful discussions and C. Richter for help with electrical measurements. This work was supported by Deutsche Forschungsgemeinschaft, FOR 520.

[1] Y. Tokura, Rep. Prog. Phys. **69**, 797 (2006).
[2] E. Dagotto *et al.*, Phys. Rep. **344**, 1 (2001).
[3] K. Dörr, J. Phys. D **39**, R125 (2006).
[4] R. von Helmolt *et al.*, Phys. Rev. Lett. **71**, 2331 (1993).
[5] Z. Fang *et al.*, Phys. Rev. Lett. **84**, 3169 (2000).
[6] Yafeng Lu *et al.*, Phys. Rev. B **73**, 184406 (2006).
[7] C. Thiele *et al.*, Phys. Rev. B **75**, 054408 (2007); Appl. Phys. Lett. **87**, 262502 (2005).
[8] M. Ziese *et al.*, Phys. Rev. B **68**, 134444 (2003).
[9] R. Lengsdorf *et al.*, Phys. Rev. B **69**, 140403 (2004); Phys. Rev. B **75**, 180401 (2007).
[10] P. M. Raccah *et al.*, Phys. Rev. **155**, 932 (1967).
[11] D. M. Sherman, in *Advances in Physical Geochemistry*, edited by S. K. Saxena (Springer-Verlag, Berlin, 1988).
[12] M. A. Korotin *et al.*, Phys. Rev. B **54**, 5309 (1996).
[13] M. A. Rodriguez *et al.*, J. Solid State Chem. **118**, 323 (1995).
[14] D. Louca *et al.*, Phys. Rev. Lett. **91**, 155501 (2003).
[15] Masayuki Itoh *et al.*, J. Phys. Soc. Jpn. **63**, 1486 (1994).
[16] R. Caciuffo *et al.*, Phys. Rev. B **59**, 1068 (1999).
[17] M. Kriener *et al.*, Phys. Rev. B **69**, 094417 (2004).
[18] J. Wu *et al.*, Phys. Rev. Lett. **94**, 037201 (2005).
[19] D. Phelan *et al.*, Phys. Rev. Lett. **96**, 027201 (2006).
[20] D. Fuchs *et al.*, Physica (Amsterdam) **B349**, 337 (2004); Phys. Rev. B **71**, 092406 (2005).
[21] R. Gangineni *et al.*, Appl. Phys. Lett. **91**, 122512 (2007).
[22] H. M. Aarbogh *et al.*, Phys. Rev. B **74**, 134408 (2006).
[23] Hai-Wen Hsu *et al.*, Jpn. J. Appl. Phys. **39**, 61 (2000).
[24] Masatoshi Imada *et al.*, Rev. Mod. Phys. **70**, 1039 (1998).
[25] G. Maris *et al.*, Phys. Rev. B **67**, 224423 (2003).
[26] M. J. R. Hoch *et al.*, Phys. Rev. B **75**, 104421 (2007).
[27] J. Sunstrom *et al.*, J. Solid State Chem. **139**, 388 (1998).
[28] J. Cao *et al.*, Phys. Rev. Lett. **90**, 157601 (2003).